PHYSICAL REVIEW B **72**, 195320 (2005)

Kinetic origin of island intermixing during the growth of Ge on Si(001)

G. Katsaros,* G. Costantini, M. Stoffel, R. Esteban, A. M. Bittner, A. Rastelli, U. Denker, O. G. Schmidt, and K. Kern
Max-Planck-Institut für Festkörperforschung, Heisenbergstrasse 1, D-70569 Stuttgart, Germany
(Received 5 July 2005; revised manuscript received 26 August 2005; published 11 November 2005)

The effects of substrate temperature, growth rate, and postgrowth annealing on the composition of Ge islands grown on Si(001) were investigated with a combination of selective wet chemical etching and atomic force microscopy. A simple kinetic model comprising only surface diffusion processes can explain all the experimentally observed compositional profiles for pyramid and dome islands grown in the 560–620 °C range. From this model three-dimensional compositional maps were extracted. By performing annealing experiments a change in the composition of the domes was observed. This could be explained as the result of the islands' movement induced by alloying-driven energy minimization. Also in this case kinetically hindered bulk diffusion processes are not needed to explain the experimental observations.

DOI: 10.1103/PhysRevB.72.195320 PACS number(s): 68.65.Hb, 81.15.Hi, 81.65.Cf

I. INTRODUCTION

Self-organized semiconductor nanostructures are the subject of intense investigations since they may act as building blocks for future nanoscale applications such as quantum computing and optoelectronic devices. In particular, the interest in SiGe quantum dots (QDs) raised continuously during the past 15 years following the original discovery that dislocation-free islands can be formed by depositing a few monolayers (ML) of Ge on Si(001).[1,2]

The optoelectronic properties of self-organized semiconductor QDs are strongly influenced by their morphology, strain, and composition, which are interrelated. In the last few years there has been a significant amount of work by means of scanning tunneling microscopy characterizing the early stages of Ge epitaxial growth on Si(001),[3,4] the formation of islands,[5–8] and the transition between different island types.[9–11] There have also been detailed studies on the morphological changes occurring during Si capping,[12–14] which is important in view of device applications. The strain status of freestanding islands has been addressed by diffraction methods,[15] ultrasonic force microscopy,[16] and electron microscopy.[17] The majority of the studies concerning the QD composition relied on diffractive[18–20] or spectroscopic techniques[21–24] that give an average value over a large number of islands. They are therefore restricted to samples with a monomodal island distribution and they do not allow the addressing of individual islands so as to investigate compositional variations from island to island. More recently, electron[25] and x-ray microscopy based[26] experiments were performed for measuring compositional variations throughout individual dots. An alternative method that combines selective chemical etching and atomic force microscopy (AFM) has recently been used by Schmidt *et al.*[27] and Denker *et al.*[28] in order to probe the composition of Ge hut clusters and pyramids in single and stacked layers. Just recently, Malachias *et al.*[29] and Schülli *et al.*[30] used the same procedure together with a set of diffraction techniques to study monomodal distributions of dome islands.

Despite all these works, a general treatment of the QD composition problem giving a coherent description of the different reported results is still missing. Moreover, it is still debated whether the observed compositional profiles are originating from bulk interdiffusion phenomena triggered by the nonuniform stress fields[25,31–33] or from surface mediated diffusion processes.[26–28,34] In the present paper we investigate the dependence of the composition of Ge islands on the main growth parameters by varying the substrate temperature, the growth rate, and the annealing time. Based on our experimental results, we propose a unified description of the SiGe alloying during the growth of pyramids and domes. The nonuniform compositional profiles of the islands can be described within a very simple kinetic growth model that involves only surface diffusion processes. Also the compositional changes occurring after the island annealing can be explained in terms of pure surface diffusion, thus demonstrating that, at our experimental temperatures, thermodynamically driven bulk intermixing is not necessary for explaining the islands' compositions.

II. METHODS

The samples used for this study were grown by solid source molecular beam epitaxy. After chemical cleaning and deoxidation at 950 °C in ultrahigh vacuum, a 100 nm thick Si buffer was grown while ramping the substrate temperature from 480 °C to the island growth temperature (560–620 °C). The samples were grown by depositing 6 ML of Ge at a rate of 0.04 ML/s. After the formation of a planar wetting layer (WL), the appearance of three-dimensional (3D) islands was monitored by reflection high energy electron diffraction. Two samples grown at 580 °C were subsequently *in situ* annealed at the same temperature for 10 and 20 minutes, respectively. So as to investigate the effect of the growth rate, another set of samples was prepared by depositing 11 ML of Ge with growth rates of 0.04 ML/s and 0.08 ML/s. The etching experiments were performed at room temperature by dipping the samples for 10 minutes in a commercial (Merck) 31% hydrogen peroxide (H_2O_2) solution, which is known to etch selectively Ge over Si and to stop etching for SiGe alloys with Ge concentrations less than 65%.[27] Longer etching times did not significantly change the morphology of the remaining structures. After being etched,

 ©2005 The American Physical Society

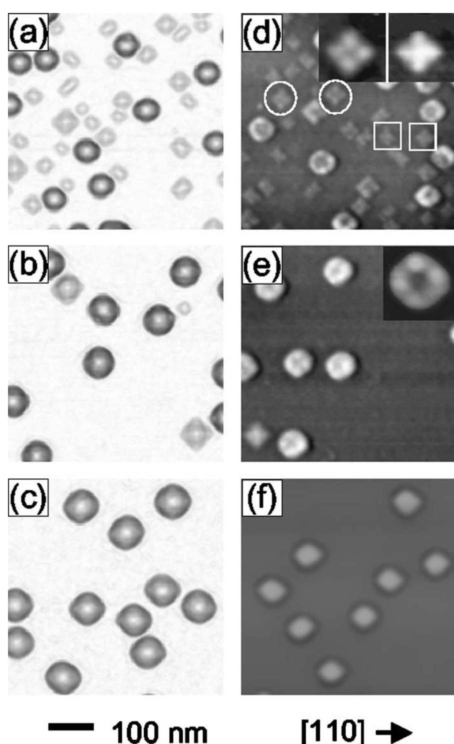

FIG. 1. AFM topographies showing the morphology of Ge islands grown on Si(001) before (left column) and after 10 minutes of 31% H_2O_2 etching (right column). The growth temperatures are 580 °C for (a) and (d), 600 °C for (b) and (e) and 620 °C for (c) and (f). The insets show a higher magnification (80×80 nm^2) of (d) the two different observed etched structures for pyramid islands, and (e) the protrusions in the ring structures of the etched domes. The encircled islands in (d) are examples of pyramids without apex while the ones enclosed by squares correspond to pyramids with apex. The gray scale in (a)–(c) is related to the local surface slope while in (d)–(f) it represents a combination of local surface height and gradient so as to enhance small-scale morphological details.

the samples were rinsed in deionized water and their morphology was investigated by means of AFM in tapping mode.

To gain a better understanding of the experimental observations, we performed growth simulations similar to those reported in Ref. 28. In the present work we additionally included the influence of the substrate temperature by taking into account a higher Si diffusivity and a larger Si content in the WL[35] for higher temperatures.

III. AS-GROWN SAMPLES

A. Effect of growth temperature

Figures 1(a)–1(c) show AFM topographies of QD samples grown at 580 °C, 600 °C, and 620 °C, respectively. With increasing growth temperature, the size of the islands increases and their density decreases, as expected. The sample grown at 580 °C shows a coexistence of hut clusters (elongated islands bounded by four {105} facets and edges parallel to the [100] directions),[2] pyramids (similar to the hut clusters but with a square base and generally larger) and domes (multifaceted islands with steeper facets).[36] At 600 °C we observe mainly domes and transition islands[11] while at 620 °C the surface is covered by a monomodal distribution of domes. The right column of Fig. 1 shows the corresponding surface morphologies after the chemical etching in a 31% H_2O_2 solution. The huts become shallower[27] and the pyramids show a crosslike shape, as has been already reported previously[28] [left inset in Fig. 1(d)]. The selectivity of the etchant implies that the remaining parts of the islands (in the case of pyramids, the corners) have a larger Si content. Etched domes exhibit a ringlike structure up to a temperature of 600 °C. At 620 °C the rings transform into a convex moundlike structure, which occurs also at higher growth temperatures.[30] The 560 °C sample (not shown) is very similar to that grown at 580 °C, both before and after etching.

A careful inspection of the etched pyramids grown at 560 °C and 580 °C reveals that a few of them do not exhibit the characteristic cross shape but still have a protruding apex [left and right inset in Fig. 1(d), respectively]. This observation indicates that these latter pyramids have an increased Si content at their top. In order to interpret this difference and to derive a complete 3D compositional map for the two types of pyramids, we performed simulations similar to those reported in Ref. 28. They were done for a large range of diffusion lengths and WL compositions so as to investigate their effect on the final composition of the islands.

For each set of parameters, more than 200 simulations were performed and their results were averaged so as to obtain a composition value for each different part of the pyramid.[28] Figure 2(a) shows a two-dimensional (2D) cross section through such a compositional map along the [100] direction for a pyramid with an high Ge composition and a Si diffusion length equal to 25% of the pyramid base. For a direct comparison with the etching experiments, we have to consider all the points of this map with a Ge composition lower than 65%, a so-called 65% Ge isocompositional profile. This is shown in Fig. 2(b), which agrees fairly well with the experimental crosslike structure shown in Fig. 2(c). If we consider a pyramid with a higher average Si content, a different result is obtained: the isocompositional profile is now showing a protruding apex [Fig. 2(e)], in good agreement with the second type of experimentally observed etched pyramids [Fig. 2(f)]. To understand the origin of this phenomenon we have to consider that, as recently demonstrated,[11] pyramids grow by a successive overlay of {105} facets, involving predominantly surface processes. During the formation of a new {105} facet, the probability that a Si atom is incorporated at a certain position is thus proportional to the probability that it reaches that position by diffusing from the WL. As a consequence, we can assume that the composition of each part of the island is mainly determined at the moment of its growth. Points *A* and *B* in Fig. 2(g) were incorporated into the pyramid at different times at which the pyramid had different sizes. The distance Si atoms had to travel for reaching *A* is on average larger than for *B*, resulting in a higher Si composition of *B* (pyramid center) with respect to *A*. Evidently, the geometrical argument presented above is true also for Ge atoms. However, it has been shown that the diffusion length of Ge is larger than that of Si,[37] and furthermore the latter has to

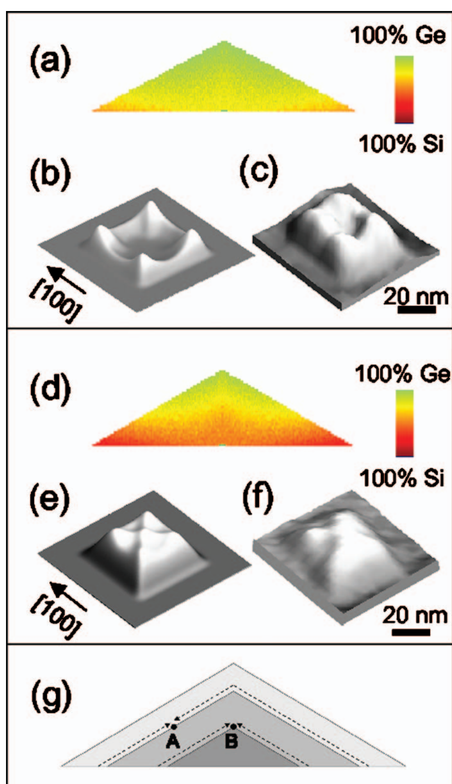

FIG. 2. (Color) (a) 2D cross section through the compositional map of a simulated pyramid with a Si diffusion length corresponding to 1/4 of its base and an average Ge composition of 75%. The cross section is along [100], i.e., along the pyramid side and passes through its center. (b) 65% Ge isocomposition surface profile of the same pyramid. For comparing the simulated data with the AFM images, the former were smoothened by means of a Gaussian convolution. (c) Experimental etched structure of a pyramid without apex. (d) Same as (a) but with an average Ge composition 52%. (e) 65% Ge isocomposition surface profile of the pyramid in (d). (f) Experimental etched structure of a pyramid with protruding apex. (g) Schematic representation for the origin of the higher Si content close to the pyramid center. The arrows indicate the path that atoms starting from the WL have to follow in order to reach different positions of the pyramid at different moments of the pyramid growth. See text for details.

diffuse out of the thin WL before diffusing towards the islands. Thus, the motion of the Ge atoms, due to their larger diffusivity, is not significantly restricted by this geometrical effect. The increase of the Si content in the center is always present but it appears more clearly for a higher overall Si composition [compare Figs. 2(a) and 2(d)]. This result implies that those pyramids, which after etching still have a protruding central part, also have a higher total Si content. In other words, although the pyramids look morphologically identical before etching, *they do not have the same composition*. This could be caused by local fluctuations of the WL composition[38] induced by the nonuniform distribution and density of the islands.

The etched domes grown in the 560–600 °C temperature range show a ringlike structure, whose height increases with increasing temperature: at 560 °C it is of 1.4 nm, at 580 °C of 3.6 nm, and at 600 °C of 6.5 nm. This implies that also in

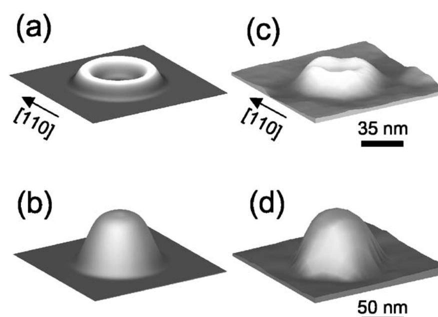

FIG. 3. (Left column) Simulated 65% Ge isocompositional surface profiles for (a) a dome with small Si content and diffusion length and (b) a dome with a higher Si content and diffusion length. For comparing the simulated data with the AFM images, the former were smoothened by means of a Gaussian convolution. A circular shape for the base of the dome was assumed for simplicity. (c) and (d) experimental etched structures of domes grown at 580 °C and 620 °C, respectively.

the case of domes, the periphery has a higher Si content compared to the center. The actual difference is that while for the square-based pyramids the Si-richer regions are mainly concentrated in the corners,[28] this geometrical effect is almost absent for the domes which have a much more symmetric octagonal base.[36] Nevertheless, a careful inspection reveals that for many of the domes a tiny modulation of the ring does exist in the form of four protrusions, located at the same position of the pyramids' corners [inset in Fig. 1(e)]. This can be easily understood when considering that domes evolve from pyramids through a transformation that involves primarily surface processes.[11] It is thus not surprising that the composition of a dome "remembers" that of the pyramid from which it has originated.

At 620 °C the ring is replaced by a convex mound structure having a height of about 13 nm [Fig. 1(f)]. A qualitatively similar compositional profile was recently reported by Malachias *et al.*[29] for Ge domes grown by chemical vapor deposition. In order to rationalize this change we have to consider that the increase of the substrate temperature has two main effects. First, it augments the Si content of the WL[35] and second, it increases the adatom surface diffusivity. This is particularly important for Si atoms, since the diffusion of Ge atoms is already activated at lower temperatures.[11] As a consequence, at higher temperatures more Si atoms can reach even high-lying points of the island, thus producing a "Si-filling" of the central hole and creating the mound structure. By including these two effects into the growth simulations for dome-shaped islands, the transition from a ring- to a moundlike isocompositional profile can indeed be reproduced rather well (Fig. 3). This result further confirms that the inhomogeneous Si distribution of islands grown at lower temperatures is produced by kinetic limitations. Moreover, it demonstrates the generality of our simple model and proves that bulk diffusion driven by stress fields is not necessary for justifying the experimentally observed compositional profiles.

For even higher temperatures the simulations show that Si atoms can access every point of the island with high prob-

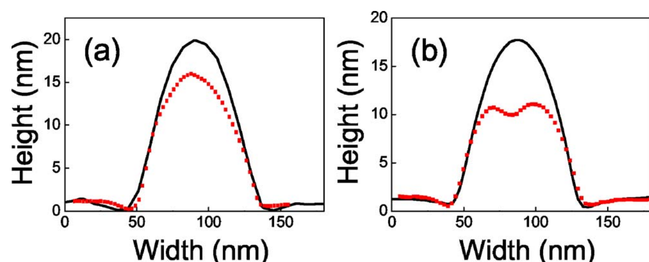

FIG. 4. (Color online) Representative AFM linescans of domes grown at 620 °C with two different growth rates: (a) 0.04 ML/s and (b) 0.08 ML/s before (solid black line) and after (dotted red line) selective chemical etching.

ability, producing a more uniform and Si-richer alloying of the island. This agrees well with the experimental report by Schülli *et al.*[30] that the dome islands grown at 700 °C are almost not affected by the etching in a 31% H_2O_2 solution.

B. Effect of the growth rate

The effect of the growth rate on the island composition was investigated by growing 11 ML of Ge at a fixed substrate temperature (620 °C) but with different deposition rates, 0.04 and 0.08 ML/s, respectively. The samples are characterized in both cases by a monomodal distribution of domes, but their composition appears to be different. In the first sample the etched islands show a moundlike structure with an average height of 14.6±0.7 nm, while in the second they show a ringlike profile with a height of 10.1±1.3 nm (Fig. 4). The influence of the Ge growth rate on the island composition can be also understood within a kinetically determined growth model. In fact, while the Ge supply rate for a growing island is doubled, that of Si remains almost unchanged, being principally determined by the sample temperature. This leads to a back transformation of the etched morphologies from mound to ringlike structures as also verified by the simulation.

Summarizing, we have so far demonstrated that a simple kinetic growth model can qualitatively reproduce the complex inhomogeneous alloying of self-organized 3D islands. Despite its simplicity, the model is able to grasp the essential features of the compositional profiles of pyramids as well as domes and it correctly describes their evolution as a function of the substrate temperature and of the growth rate. Its basic assumptions are clearly oversimplified and other important effects (strain release, surface energy, etc.) should be included in a true comprehensive description of the island growth. For example, the kinetic accumulation of Si at the pyramid edges could possibly be amplified due to the energy gain that Si atoms experience when attaching to already Si-rich regions. Nevertheless, the good agreement with the experimental results lets us expect that, even by taking into account these further effects, the main origin for the measured composition profiles would still be of a kinetic nature.

IV. ANNEALED SAMPLES

An important procedure in the growth of self-organized quantum dots is the so-called growth interruption, by which

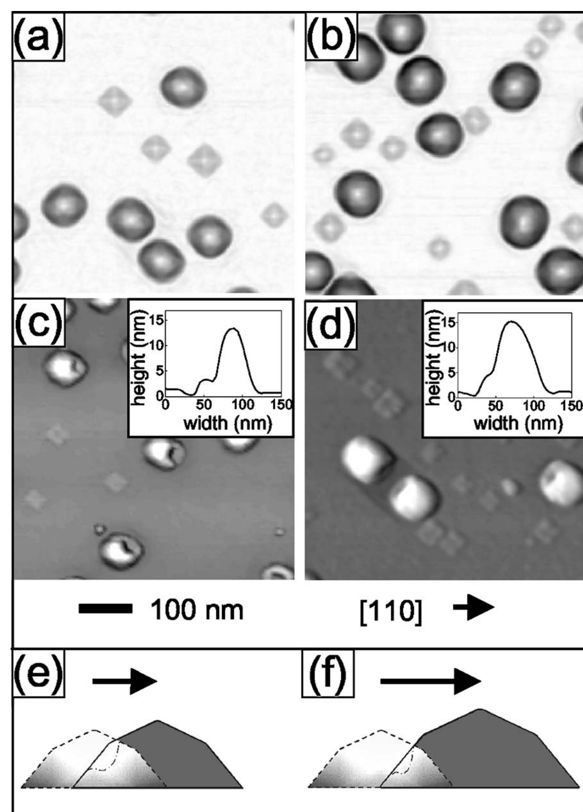

FIG. 5. AFM topographies showing the morphology of annealed Ge islands before (upper row) and after (lower row) 10 minutes of 31% H_2O_2 etching. The annealing times are 10 minutes for (a) and (c) and 20 minutes for (b) and (d). The insets in (c) and (d) show a representative line scan across the etched islands. The gray scale in (a) and (b) is related to the local surface slope while in (c) and (d) it represents a combination of local surface height and gradient so as to enhance small-scale morphological details. (e) and (f) represent a schematic model of the island movement and of its effect on the island composition. The dashed border includes the original island and its compositional profile taken from the actual simulation (darker regions are Si rich and not attacked by the etchant). The dashed-dotted line inside the final island indicates the line scan that is expected after etching. The arrows indicate the direction and the “magnitude” of the island motion.

the sample is kept at the growth temperature for a certain time after the deposition flux has been stopped. To investigate its effect on the island composition, we annealed samples grown at 580 °C for 10 and 20 minutes (Fig. 5). The comparison between Fig. 1(a) and Figs. 5(a) and 5(b) reveals that a coarsening process has taken place in which the hut clusters have disappeared and the average island size has increased. After annealing, the etched pyramids show qualitatively the same compositional profile as the as-grown ones.

Conversely, the domes display a completely different compositional profile after the growth interruption (for both 10 and 20 minutes). The symmetric Si-rich ring is replaced by a strongly asymmetric structure in which the part removed by the etching is close to the island border. Moreover, line scans as those shown in the insets of Figs. 5(c) and 5(d) reveal that the Ge-rich part of these domes becomes smaller

with increasing annealing time. These very peculiar compositional profiles cannot be easily explained without considering that Ge islands move laterally during annealing. Denker *et al.*[39] recently demonstrated for samples grown at 740 °C that an initial fluctuation of material on one side of an island (possibly caused by the elastic repulsion between neighboring islands)[40] can initiate a self-sustaining lateral movement. This instability derives from the energy gain that Ge atoms experience when migrating from the receding to the advancing side of the island where they can intermix with Si originating from the WL. The islands are thus growing in size while moving and their advancing front has a higher Si content.[39] Figure 5(e) schematically shows the effect of this movement on the composition of domes that initially had a Si-rich ring. The right side of the island is highly alloyed and will therefore not be affected by the etchant. The left side is constituted by the material of the original island with a lower lying Si-rich region that corresponds to the original ring and a higher lying Ge-rich part that will be removed after etching. The total resulting compositional profile is thus very similar to the experimentally measured one [see line scan in inset of Fig. 5(c)]. The observation that the island displacement scales with the annealing time[39] further explains why the etched part of the island becomes smaller for longer growth interruptions [Fig. 5(f)]. For islands close to each other, we observe a clear correlation between the direction of motion and the direction away from the nearest neighbor. A very similar behavior is also seen when the annealing is performed at higher temperatures,[39] and supports the above interpretation.

Since the compositional profile of pyramids is qualitatively the same for the as-grown and the annealed islands, a movement seems not to be plausible in this case. The origin of the different behavior of pyramids and domes cannot be unambiguously derived from our experiments. One reason could be that in the case of pyramids the repulsive strain fields needed to trigger the island motion[39] are not strong enough.[41]

V. DISCUSSION AND CONCLUSION

By comparing our results with the compositional profiles reported in the literature, we notice that there is a good agreement on the observation that the composition of the dots becomes richer in Ge closer to the apex of the islands[18–25,29] and that the overall Si content is increasing with increasing growth temperature.[22,30] In the majority of these studies, experimental techniques which integrate over a large number of dots were used. As a consequence, it was not possible to detect compositional fluctuations among different islands, nor to extract precise 3D compositional profiles with high lateral resolution as can be done by combining atomic force microscopy and selective chemical etching.

Recently Malachias *et al.*[29] obtained a detailed 3D map of the Si and Ge distribution within dome islands by using grazing incidence anomalous x-ray scattering. Their reported experimental profile fits well with the moundlike structure described in Sec. III and we therefore believe that it could be explained by a growth model similar to that presented here. By combining transmission electron microscopy and electron energy-loss spectroscopy, Floyd *et al.*[25] investigated the composition of dome islands with both lateral and height resolution. Although they expected a lateral modulation in the island composition caused by a strain-driven bulk interdiffusion, they did not observe it. A possible reason could be that small variations are not detected by a transmission technique that integrates over 100–200 nm thick sample slices. In our study, for nominally similar growth temperatures, we do observe lateral variations in the island composition in the form of ring structures for domes and of crosslike structures for pyramids. Nevertheless, the growth model we have introduced to explain these effects is based just on surface processes and does not need to take into account any bulk interdiffusion. This is supported by the values of the corresponding energy barriers reported in the literature:[42–44] according to them, in the 560–620 °C temperature range, bulk interdiffusion is kinetically limited and much too small to explain the amount of Si that we observe in the islands. Thus, bulk interdiffusion should not be considered as the main factor responsible for island intermixing.

In conclusion, in this work we have investigated the dependence of the composition of self-organized islands on the temperature, the growth rate, and the annealing time. We were able to explain all the observed compositional profiles of the as-grown islands within a very simple model that is of kinetic origin and relies just on surface diffusion phenomena. Based on these arguments we were able to propose a compositional map for both pyramids and domes and to explain the asymmetric profiles of the annealed domes.

ACKNOWLEDGMENTS

The authors would like to thank N. Y. Jin-Phillipp, C. Manzano, and P. Acosta-Diaz for helpful discussions. G. K. acknowledges the financial support of DAAD (Deutscher Akademischer Austausch Dienst).

*Corresponding author. Email address: g.katsaros@fkf.mpg.de

[1] D. J. Eaglesham and M. Cerullo, Phys. Rev. Lett. **64**, 1943 (1990).
[2] Y. W. Mo and M. G. Lagally, Mater. Sci. Eng., B **14**, 311 (1992).
[3] U. Köhler, O. Jusko, B. Müller, M. Horn-von Hoegen, and M. Pook, Ultramicroscopy **42–44**, 832 (1992).
[4] B. Voigtländer and M. Kästner, Phys. Rev. B **60**, R5121 (1999).
[5] I. Goldfarb, P. T. Hayden, J. H. G. Owen, and G. A. D. Briggs, Phys. Rev. Lett. **78**, 3959 (1997).
[6] A. Vailionis, B. Cho, G. Glass, P. Desjardins, David G. Cahill, and J. E. Greene, Phys. Rev. Lett. **85**, 3672 (2000).
[7] D. E. Jesson, M. Kästner, and B. Voigtländer, Phys. Rev. Lett. **84**,

330 (2000).

[8] J. Tersoff, B. J. Spencer, A. Rastelli, and H. von Känel, Phys. Rev. Lett. **89**, 196104 (2002).

[9] G. Medeiros-Ribeiro, A. M. Bratkovski, T. I. Kamins, D. A. A. Douglas, A. A. Ohlberg, and R. S. Williams, Science **279**, 353 (1998).

[10] F. M. Ross, R. M. Tromp, and M. C. Reuter, Science **286**, 1931 (1999).

[11] F. Montalenti, P. Raiteri, D. B. Migas, H. von Känel, A. Rastelli, C. Manzano, G. Costantini, U. Denker, O. G. Schmidt, K. Kern, and L. Miglio, Phys. Rev. Lett. **93**, 216102 (2004).

[12] P. Sutter and M. G. Lagally, Phys. Rev. Lett. **81**, 3471 (1998).

[13] A. Rastelli, M. Kummer, and H. von Känel, Phys. Rev. Lett. **87**, 256101 (2001).

[14] A. Rastelli, E. Müller, and H. von Känel, Appl. Phys. Lett. **80**, 1438 (2002).

[15] A. J. Steinfort, P. M. L. O. Scholte, A. Ettema, F. Tuinstra, M. Nielsen, E. Landemark, D.-M. Smilgies, R. Feidenhans'l, G. Falkenberg, L. Seehofer, and R. L. Johnson, Phys. Rev. Lett. **77**, 2009 (1996).

[16] Oleg V. Kolosov, M. R. Castell, C. D. Marsh, G. A. Briggs, T. I. Kamins, and R. S. Williams, Phys. Rev. Lett. **81**, 1046 (1998).

[17] C.-P. Liu, J. M. Gibson, D. G. Cahill, T. I. Kamins, D. P. Basile, and R. S. Williams, Phys. Rev. Lett. **84**, 1958 (2000).

[18] R. Magalhães-Paniago, G. Medeiros-Ribeiro, A. Malachias, S. Kycia, T. I. Kamins, and R. S. Williams, Phys. Rev. B **66**, 245312 (2002).

[19] T. U. Schülli, J. Stangl, Z. Zhong, R. T. Lechner, M. Sztucki, T. H. Metzger, and G. Bauer, Phys. Rev. Lett. **90**, 066105 (2003).

[20] J. Stangl, A. Daniel, V. Holý, T. Roch, G. Bauer, I. Kegel, T. H. Metzger, Th. Wiebach, O. G. Schmidt, and K. Eberl, Appl. Phys. Lett. **74**, 1474 (2001).

[21] F. Boscherini, G. Capellini, L. Di Gaspare, F. Rosei, N. Motta, and S. Mobilio, Appl. Phys. Lett. **76**, 682 (2000).

[22] G. Capellini, M. De Seta, and F. Evangelisti, Appl. Phys. Lett. **78**, 303 (2001).

[23] N. Motta, F. Rosei, A. Sgarlata, G. Capellini, G. Mobilio, and F. Boscherini, Mater. Sci. Eng., B **88**, 264 (2002).

[24] A. V. Kolobov, H. Oyanagi, S. Wei, K. Brunner, G. Abstreiter, and K. Tanaka, Phys. Rev. B **66**, 075319 (2002).

[25] M. Floyd, Y. T. Zhang, K. P. Driver, J. Drucker, P. A. Crozier, and D. J. Smith, Appl. Phys. Lett. **82**, 1473 (2003).

[26] F. Ratto, F. Rosei, A. Locatelli, S. Cherifi, S. Fontana, S. Heyn, P.-D. Szkutnik, A. Sgarlata, M. De Crescenzi, and N. Motta, J. Appl. Phys. **97**, 043516 (2005).

[27] O. G. Schmidt, U. Denker, S. Christiansen, and F. Ernst, Appl. Phys. Lett. **81**, 2614 (2002).

[28] U. Denker, M. Stoffel, and O. G. Schmidt, Phys. Rev. Lett. **90**, 196102 (2003).

[29] A. Malachias, S. Kycia, G. Medeiros-Ribeiro, R. Magalhães-Paniago, T. I. Kamins, and R. S. Williams, Phys. Rev. Lett. **91**, 176101 (2003).

[30] T. U. Schülli, M. Stoffel, A. Hesse, J. Stangl, R. T. Lechner, E. Wintersberger, M. Sztucki, T. H. Metzger, O. G. Schmidt, and G. Bauer, Phys. Rev. B **71**, 035326 (2005).

[31] T. I. Kamins, G. Medeiros-Ribeiro, D. A. A. Ohlberg, and R. S. Williams, Appl. Phys. A **67**, 727 (1998).

[32] X. Z. Liao, J. Zou, D. J. H. Cockayne, J. Qin, Z. M. Jiang, X. Wang, and R. Leon, Phys. Rev. B **60**, 15605 (1999).

[33] S. A. Chaparro, J. Drucker, Y. Zhang, D. Chandrasekhar, M. R. McCartney, and D. J. Smith, Phys. Rev. Lett. **83**, 1199 (1999).

[34] N. Liu, J. Tersoff, O. Baklenov, A. L. Holmes, Jr., and C. K. Shih, Phys. Rev. Lett. **84**, 334 (2000).

[35] G. Katsaros, A. Rastelli, M. Stoffel, P. Acosta-Diaz, O. G. Schmidt, G. Costantini, and K. Kern (unpublished).

[36] A. Rastelli and H. von Känel, Surf. Sci. **515**, L493 (2002).

[37] V. Cherepanov and B. Voigtländer, Phys. Rev. B **69**, 125331 (2004).

[38] F. Ratto, F. Rosei, A. Locatelli, S. Cherifi, S. Fontana, S. Heun, P.-D. Szkutnik, A. Sgarlata, M. De Crescenzi, and N. Motta, Appl. Phys. Lett. **84**, 4526 (2004).

[39] U. Denker, A. Rastelli, M. Stoffel, J. Tersoff, G. Katsaros, G. Costantini, K. Kern, N. Y. Jin-Phillip, D. E. Jesson, and O. G. Schmidt, Phys. Rev. Lett. **94**, 216103 (2005).

[40] M. Stoffel, A. Rastelli, S. Kiravittaya, and O. G. Schmidt, Phys. Rev. B (to be published).

[41] P. Raiteri, L. Miglio, F. Valentinotti, and M. Celino, Appl. Phys. Lett. **80**, 3736 (2002).

[42] J. Räisänen, J. Hirvonen, and A. Antilla, Solid-State Electron. **24**, 333 (1981).

[43] G. L. McVay and A. R. DuCharme, J. Appl. Phys. **44**, 1409 (1973).

[44] J. Wan, Y. H. Luo, Z. M. Jiang, G. Lin, J. L. Liu, K. L. Wang, X. Z. Liao, and J. Zou, J. Appl. Phys. **90**, 4290 (2001).